

ANTI-BACTERIAL EFFECT OF MN:TiO₂ THIN FILMS SYNTHESIS BY DIP-COATING SOL-GEL METHOD

SuraY.Khalaf¹, Falah H. Ali², Yassamin Sadk Khalf³ Ali Sh. Maktoof⁴

1) Physics Department, College of Science, Mustansiriyah University, Baghdad, Iraq

2) College of science, University of Baghdad, Baghdad, Iraq

3) College of Science, Mustansiriyah University, Baghdad, Iraq

Corresponding author*:

1. sura.y.khalaf@uomustansiriyah.edu.iq

2. Falah.Ali@sc.uobaghdad.edu.iq

3. yassamin.s@uomustansiriyah.edu.iq

4. ali.sh.maktoof@uomustansiriyah.edu.iq

Article history:	Abstract:
Received: 11 th April 2025 Accepted: 10 th May 2025	<p>Manganese-doped titanium dioxide (Mn-TiO₂) has emerged as a promising material with enhanced antibacterial properties compared to pure titanium dioxide. This summary explores the key aspects of the antibacterial activity of Mn-doped titanium dioxide, counting the dip-coating sol-gel synthesis method, mechanisms of action, and factors affecting its efficacy.</p> <p>The structural tests (SIM and EFM) showed that there is a reduction in the particle size and an increase in the surface area with high homogeneity when the manganese concentration increases, as the particle size reaches 9 nanometres in the sample TM4. Visual examinations showed that there was a creep towards the visible region when the concentration of manganese increased, as the energy gap value reached 2.51 for the sample TM4. Bacterial inhibition tests showed that there is a significant inhibition upon irradiation with visible light. This is expected due to the increased surface area to volume for most samples. The best of them were selected for this application and tested for three time periods: 15, 30 and 60 minutes. This result is very important and unique, especially for medical applications.</p>

Keywords: Mn-TiO₂, Sol-gel, dip-coating, morphology, antibacterial.

INTRODUCTION

Since the discovery of the photocatalytic activity of TiO₂ [1], it has been recognized as one of the most efficient photocatalytic materials. TiO₂ is valued for its numerous properties including high photo activity, good stability, low cost, and low toxicity [2,3]. In the recent decades, TiO₂-based nanostructures gained attention have been widely studied in academic research and used in a variety of applications such as photovoltaic, sensors, removal of organic pollutants and pathogens, and energy storage [3-6]. TiO exists in three different crystalline phase which are anatase, rutile, and brookite [7]. Both Anatase and rutile possess a crystalline structure that corresponds to the tetragonal system whereas brookite has an orthorhombic crystalline structure [8]. As a bulk material, rutile is the stable phase. while, anatase is the generally preferred for solution phase preparation [9]. In 1992, the first bactericidal photocatalytic coating was developed by the Japanese Arc-Flash Company, using TiO₂ nanoparticles [10]. The Arc-Flash® photocatalytic coating displays antibacterial activity and can be used to efficiently sanitize environments including hospitals, schools, and households. In addition to be used as antimicrobial agents, TiO₂ has the potential to be used to increase product shelf-life and prevent spoilage of perishable goods by treating the air in vegetable, fruit and flower storage zone [11]. There are types of bacteria present in our daily life, including cocci, bacillus, and others. In this project the bacterium E. coli is studied. Escherichia coli bacteria is the Chapter one Theoretical part 20 predominant facultative organisms in the human gastrointestinal tract. E. coli is the type species of the genus Escherichia, which contains mostly motile gram negative bacilli within the family Enterobacteriaceae and the tribe Escherichia

Experimental Work

TiO₂ pure Preparation

TiO₂ nanoparticles were prepared by the sol-gel method. 1.2 ml of TTIP and 1.2 ml of 1- propanol (sol A), were mixed, then deionized water was added to HNO₃ (sol B) to adjust its pH (sol B), after that sol (B) was added to sol (A)

drop wise at room temperature. The solution was placed on a magnetic stirrer for 4h. The resulting solution was aged at 55 °C for 24 h, to get the final a transparent sol

Mn-doping TiO₂ preparation

Mixed was HNO₃ with deionized water to adjust the pH, (Sol A), after that sol (A) was mixed with different mole (0.01, 0.05, 0.09, 0.12 and 0.16 mol) of MnCl₂. 1.2 ml TTIP was mixed with 1.2 ml 1-propanol (Sol B). Mixture (A) was added to the mixture (B) drop by drop at room temperature. The resulting solution was stirred for 4 hours. The resulting solution was aged at 55 °C for 24 h, to get the final a transparent sol

Antibacterial Activity

The antibacterial activity of Mn-TiO₂ nanoparticles conducted a survey on Escherichia. Coli (E. coli) negative bacteria. Bacteria were measured according to McFarland Standard 0.5 which is equivalent to 1.5×10^8 in sterile Petri dishes. The diagnosed bacteria were collected by the Laboratory of Nanotechnology, Department of Biotechnology, University of Baghdad College of Sciences, using a sterile wire loop, after that a 6 mm well was drilled on the plates using a tip Sterile [11]. (25 µl) concentration from was taken 0.12 Tm4. Then it was irradiated under visible light, and then the cultivated plates containing the nanoparticles were incubated for 24 hours at 37 °C.

RESULTS AND DISCUSSION

Atomic Force Microscopy (AFM)

Figures(1) shows the, 2D, and 3D, AFM of the prepared pure and doped samples at different concentrations (0.01, 0.05, 0.09, 0.12, and 0.16) respectively, calcination at 500 °C for 2h. The results were indicative of the formation of nanoparticles in the prepared thin films samples. It was also observed that a uniform granular shaped grain was formed in all samples. The surface roughness of the pure TiO₂ structure was 5.49 nm, the average surface roughness was recorded at 6.34 nm. The roughness of the thin film surface is a criterion of its crystallinity [12]. While the surface roughness of the Mn-doped TiO₂ nano-particles was as at 0.01 mol, the roughness was 3.82 nm, the square root roughness was 4.11 nm, at 0.05 mol the surface roughness was recorded as 8.9 nm, and the roughness was recorded. The root is up to 10.4. As for shown in (Table 1) pure and Mn-doped. Is noticed that the 0.12 mol sample was the smoothest, Therefore, this sample is expected to have a very good photocatalytic activity.

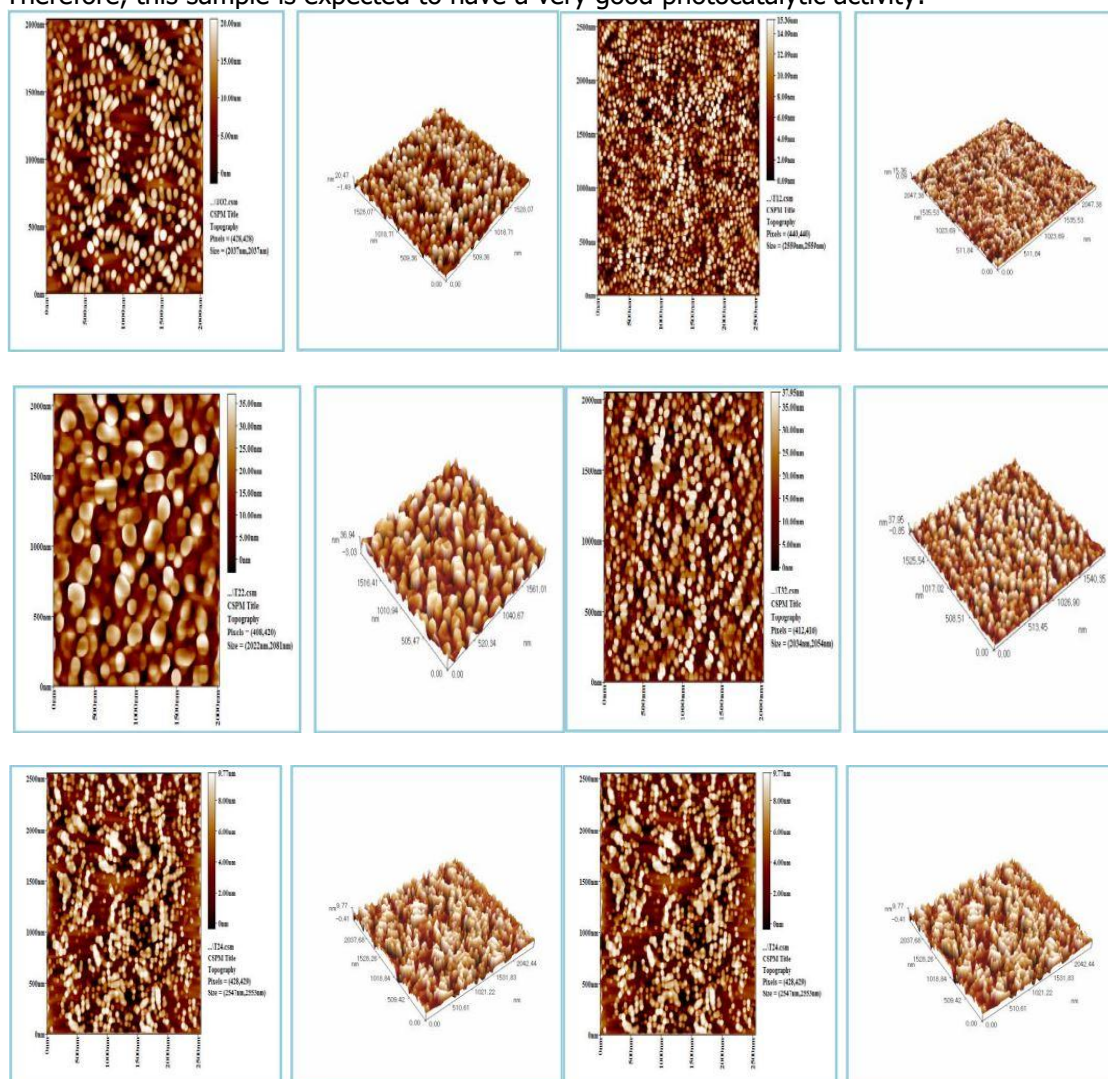


Fig 1 : 2D and 3D AFM micrographs for TiO₂ pure and Mn-doped respectively TiO₂ prepared at 500c for 2h

(1):

get

and

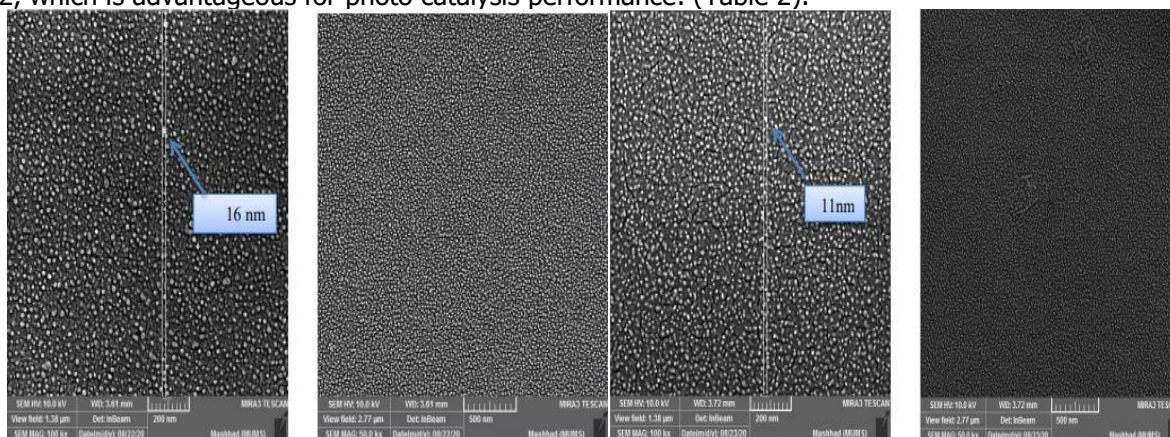
Samples	Avg. Diameter (nm)	Rms (nm)	Roughness Av(nm)	Height (nm)	Surface area ratio
T	62.74	6.34	5.49	21.9	12.2
Tm1	54.85	4.41	3.82	15.3	8.56
Tm2	84.59	10.4	8.93	39.7	13.7
Tm3	59.83	11.2	9.7	38.7	38.3
Tm4	75.79	2.94	2.54	10.1	1.16
Tm5	99.18	2.95	2.92	11.5	2.27

doped samples

Table
the
AFM
data
that
for TiO_2
pure
Mn-

Scanning Electron Microscopy (SEM)

The surface profile and particle size of the prepared thin films which are good for photo catalysts were determined by scanning electron microscopy (SEM). SEM images of pure and Mn-doped TiO_2 films are shown in (Figure 2) for scales (200 and 500). The common feature that can be observed in these images is the homogeneity of the particle distribution. Also, the size of the particle is very small, which is one of the most important advantages of the sol-gel technology used in the manufacture of thin films [13]. It can also be observed in some sample There is no aggregation in the sample, and the distance between the nanoparticles is very small, resulting in a significant surface area increases significantly. And therefore enhance its photocatalytic efficiency. The nanoparticle size was recorded from the scale images at (200 nm) using image analysis software, to be equal 16.24nm of pure TiO_2 . In Mn-doped TiO_2 samples the nanoparticles sizes were 11.11,12.31, 11.43nm or the Tm1, Tm2, and Tm3 samples, the values were observed, respectively, while the Tm4 sample showed a value of 9.67 (corresponding to 0.12 mol Mn), indicating greater uniformity compared to pure TiO_2 , which is advantageous for photo catalysis performance. (Table 2).



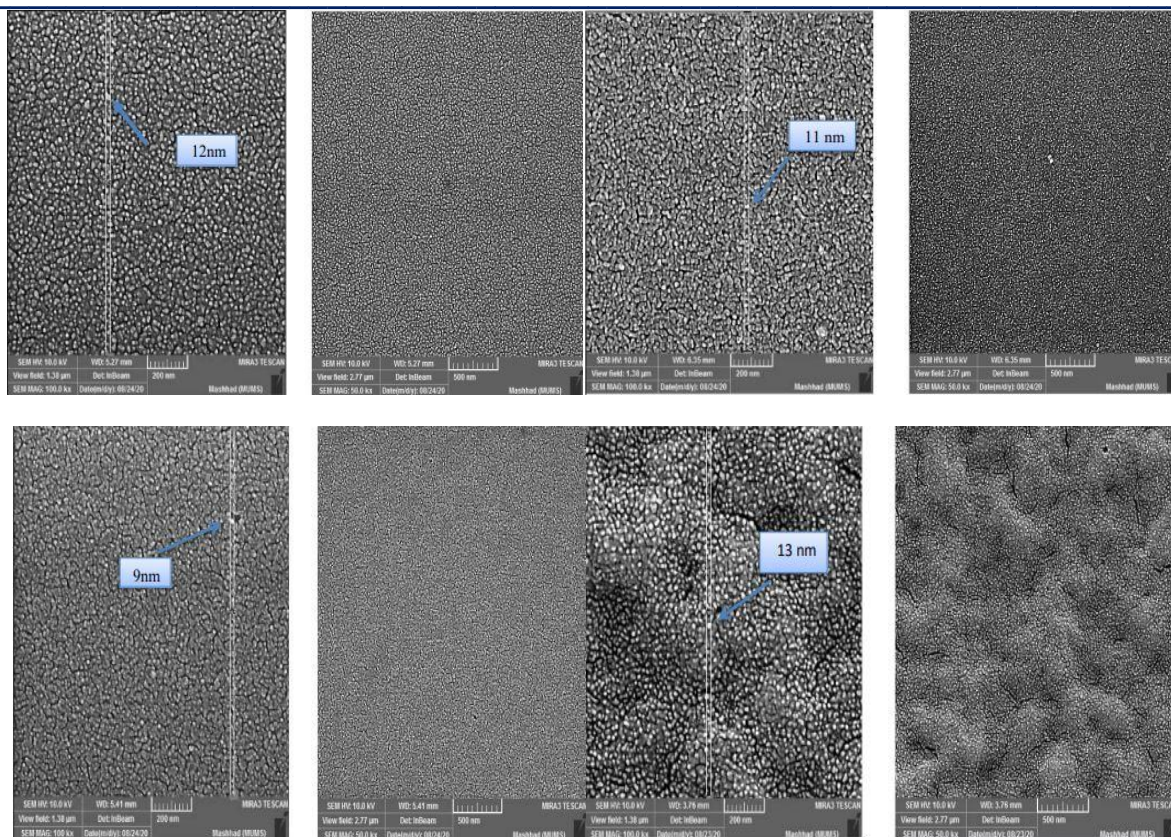
Fig 2: SEM images for pure and Mn-doped TiO₂

Table (2): The results get from SEM analysis

Samples	mol	Particle size (nm)
T	00	16
Tm1	0.01	11
Tm2	0.05	12
Tm3	0.09	11
Tm4	0.12	9
Tm5	0.16	13

Characterization of TiO₂ Optical UV-Vis Spectrophotometer

Absorption spectra were recorded for TiO₂ nanocrystalline films with different mol (0.01, 0.05, 0.09, 0.12, and 0.16mol) of Mn in the spectral range of 300-800 nm were recorded, as illustrated in Figure (3). TiO₂ mainly absorbs UV light with wavelengths shorter than 390 nm, which is according to The band gap (E_g) was determined using the following equation Planck's (eq 1).

$$E_g = \frac{hc}{\lambda} \dots\dots\dots \text{eq.1}$$

Where h is Planck's constant, c is the velocity of light, and λ is the wavelength [14].

The amount depends on the percentage of Mn increase. It can be seen that the absorption edge is 385 nm for pure TiO₂. An absorption edge is in the spectrum for the sample with the anatase phase of 0.01mol of Mn is observed at about 400 nm. Whereas, this edge was displaced at 410 nm for the sample of 0.05mol weight of Mn. A red shift was observed in the absorption spectra with the increase in the percentage of Mn by 0.09, 0.12 and 0.16, respectively. The energy gap can be defined by (Eq .1) with n = 2.

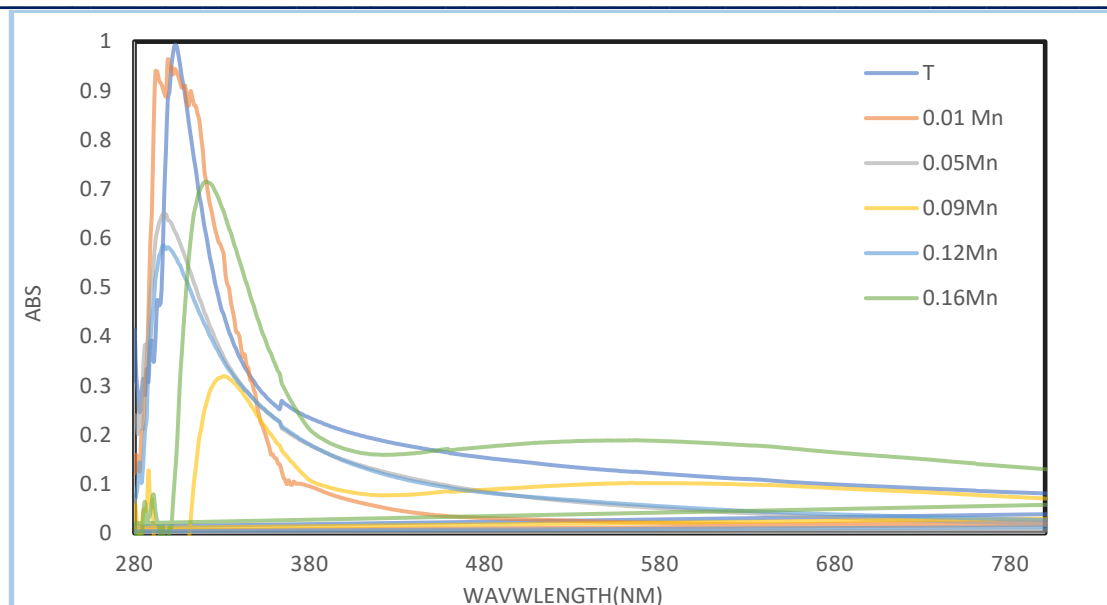


Fig. (3): Absorption spectra for the prepared samples of pure and Mn-doped TiO₂

The energy gap was found to be 3.2eV for pure nanoparticles. It was observed that with increasing manganese concentrations, the absorption edge shifted towards longer wavelengths, indicating a red shift the energy gap decreased at 0.12mol of Mn, when doping was increased, the optical absorptance has been clearly Through the spectrum of UV-Vis. And this is in line with the analysis of the optical absorption that showed that the replacement of The replacement of Ti ions with Mn ions in the TiO₂ matrix affects its properties and generally leads to reduction. the energy gap, the stable Mn oxide is Mn₂O₇, so it will be generated oxygen vacancies or interstitials of Titanium [15]. The association of mn with o leads to leaving Ti alone and this in turn leads to an Acceptor level where the probability of moving between C.B and acceptor level is greater than it is band to band transition, so we notice a decrease in the energy gap from what it is in pure TiO₂. The values for pure and Mn-doped TiO₂ are presented in Table (3)

Table (3): Band-gap values of pure and Mn-doped TiO₂ samples

Sample	Energy gap(eV)
T	3.2
Tm1	3.12
Tm2	2.9
Tm3	2.8
Tm4	2.51
Tm5	2.81

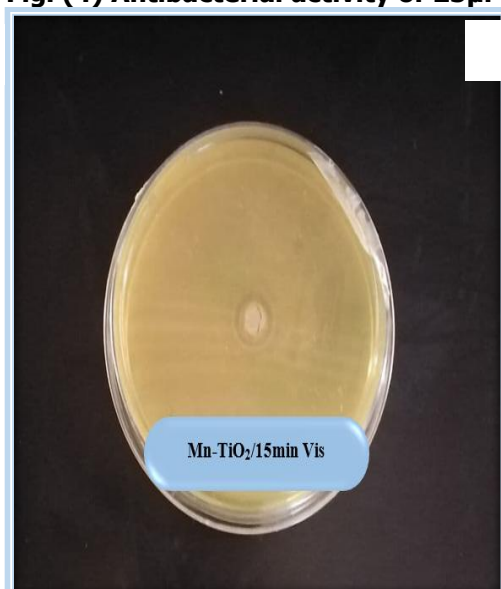
Anti-bacterial Test

The antibacterial activity of the nanoparticles was examined with E. coli in Without radiation, and visible radiation conditions with different time periods. Mn-doped TiO₂ nanoparticles was as at (0.12mol) in (figures 4 and 5), without irradiation that has no antibiotic activity is shown for this sample. while visible radiation results were Within 15 minutes the inhibition area was (4 mm) the bacteria were killed, the time was increased to 30were the inhibition area was (6 mm) the bacteria were killed, while at 60 minutes were the diameter of inhibition was(8mm) , the more irradiation, the greater the inhibition rate. Mn-TiO₂ has an excellent anti-bacterial effect in visible light. While in Mn-TiO₂ no anti-bacterial activity was detected for samples preserved in without irradiation. TM4 (0.12mol) Bacterial inhibition tests showed that there is a significant inhibition upon irradiation with visible light This is expected due to the increased surface area to volume for most samples. The best of them were selected for this application and tested for three time periods: 15, 30 and 60 minutes. This result is very important and unique, especially for medical applications.

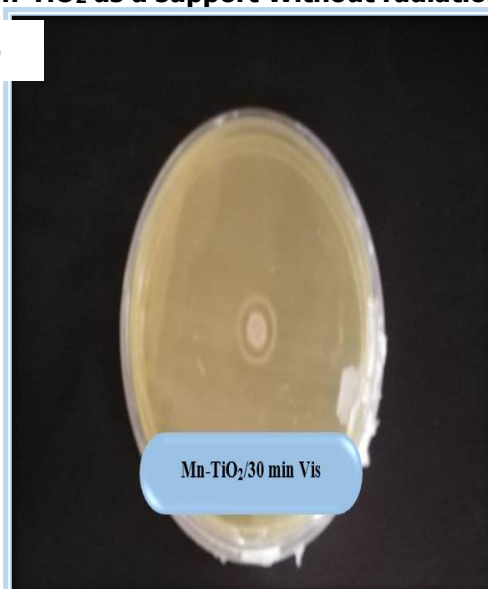


Fig. (4) Antibacterial activity of 25µl Mn-TiO₂ as a support Without radiation

a



b



c

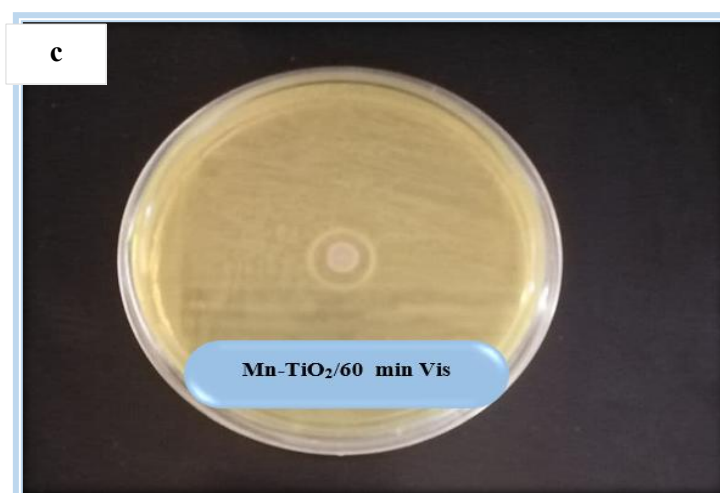


Fig. (5) Antibacterial activity of Tm4 (0.12 mol) Mn-TiO₂ as a support under Visible radiation different time (a) 15min(b) 30min(c) 60min

CONCLUSION

Nanomaterials composed of manganese and titanium dioxide have demonstrated promising Antibacterial activity against a wide range of bacteria, including both Gram-positive and Gram-negative strains, as well as multidrug-resistant bacteria. Small molecular size manganese and titanium dioxide are promising antibacterial materials with potential applications in various fields. Their unique properties and diverse mechanisms of action provide opportunities for developing effective strategies to combat bacterial infections and enhance public health.

- Funding: Not applicable.
- Ethical approval: Not applicable.

- Informed consent: Not applicable.
- Conflict of Interest: Not applicable.

REFERENCES

- [1] D. Gong, C. A. Grimes, O. K. Varghese et al., "Titanium oxide nanotube arrays prepared by anodic oxidation", *J. of Materials Research*, 16, 3331–3334, 68. (2001)
- [2] W. Wei, G. Baohua, L. Liyuan, A. H. William & D. J Wesolowski, "Synthesis of Rutile (α -TiO₂) Nanocrystals with Controlled Size and Shape by Low-Temperature Hydrolysis: Effects of Solvent Composition," *J. Phys. Chem. B*, 108, 14789-92, (2004).
- [3] Nisreen Khalid Fahad1 · Raad Saadon Sabry " Study of some mechanical and physical properties of PMMA reinforced with (TiO₂ and TiO₂-GO) nanocomposite for denture bases" *Journal of Polymer Research* (2022)
- [4] J. Sheng Hu, L., Li, W., H. Tian & S. Dai "Formation of singlecrystalline rutile TiO₂ splitting microspheres for dye-sensitized solar cells," *Solar energy*, 85(11), 2697-2703 , (2011).
- [5] M. Montazer & S. Seifollahzadeh, "Enhanced self-cleaning, antibacterial and UV protection properties of nano TiO₂ treated textile through enzymatic pretreatment," *Photochemistry and photobiology*, 87(4), 877-883 , (2011).
- [6] N. Barati, M. a F. Sani, H. Ghasemi, Z. Sadeghian, and S. M. M. Mirhoseini, *Appl. Surf. Sci.* **255**, 8328–8333 (2009).
- [7] A. M. Luís, M. C. Neves, M. H. Mendonça, and O. C. Monteiro, *Mater. Chem. Phys.* **125**, 20–25 (2011).
- [8] D. Reyes-Coronado, G. Rodríguez-Gattorno, M. E. Espinosa-Pesqueira, C. Cab, R. de Coss, and G. Oskam, *Nanotechnology* **19(14)**, 145605, (2008)
- [9] D. Nicholls, "Complexes and first-row transition elements," *Macmillan International Higher Education*, (2017)
- [10] Mathew, S., Ganguly, P., Kumaravel, V., Harrison, J., Hinder, S. J., Bartlett, J., & Pillai, S. C. Effect of chalcogens (S, Se, and Te) on the anatase phase stability and photocatalytic antimicrobial activity of TiO₂. *Materials today: proceedings*, 33, 2458-2464. (2020).
- [11] Peiris, M. M. K., Gunasekara, T. D. C. P., Jayaweera, P. M., & Fernando, S. S. N. (2018). TiO₂ nanoparticles from Baker's yeast: A potent antimicrobial.
- [12] M., Asiltürk, F., Sayılkan, & E. Arpaç, "Effect of Fe³⁺ ion doping to TiO₂ on the photocatalytic degradation of Malachite Green dye under UV and vis-irradiation," *J. of Photochemistry and Photobiology A: Chemistry*, 203(1), 64-71, 83. (2009)
- [13] E.S. Gadelwala, M.M. Koura, T.M.A. Maksoud, I.M. Elewa & H.H. Soliman, "Roughness Parameters", *J. Mater. Process. Technol.*, 123, 133-145, (2002) .
- [14] Bari R.H., Ganesan V., Potadar S & Patil L.A, "Structural, Optical and electrical properties of chemically deposited copper selenide films," *Bulletin Materials Science*, 32(1) ,37-42, (2009) .
- [15] S. Sugapriya, R. Sriram & S. Lakshmi, "Effect of annealing on TiO₂ nanoparticles," *Optik* 124 ,4971– 4975, (2013).